

# Synthesis and Crystal Structure of 1D Cd-amine Coordination Polymer and Its Luminescent Properties

XU Mengying, LIU Zhigang, FAN Ruiqing\*, GAO Song, CHEN Shuo and YANG Yulin\*

Department of Chemistry, Harbin Institute of Technology, Harbin 150001, P. R. China

**Abstract** A novel one dimension(1D) cadmium coordination polymer  $\{[\text{Cd}(\text{mpda})_3] \cdot 2(\text{NO}_3)\}_n$  (**1**) was synthesized *via* refluxing a mixture of tetradentate Schiff base ligand *N,N'*-bis(2-pyridinylethylidene)phenylene-1,3-diamine(L) and  $\text{Cd}(\text{NO}_3)_2$  in acetonitrile, whose structure was characterized by means of single crystal X-ray diffraction, FTIR spectroscopy, elemental analysis and proton nuclear magnetic resonance ( $^1\text{H}$  NMR). Center metal Cd(II) ion is six-coordinated by six nitrogen atoms from six different *m*-phenylenediamine(mpda), giving rise to a  $[\text{CdN}_6]$  octahedral coordination environment. The two adjacent cadmium centers are linked by three mpda molecules leading to the construction of 1D chain structure. The crystal structure is stabilized by N—H $\cdots$ O hydrogen bonds to form three-dimension supramolecule. Compound **1** exhibits intense yellow luminescence in solid state at 298 K ( $\lambda_{\text{em}}=554$  nm), which shows a blue shift at 77 K (*ca.* 147 nm). Additionally, fluorescence characteristics of compound **1** were investigated in different solvents (polarity: DMSO > CH<sub>3</sub>CN > CH<sub>3</sub>OH > CHCl<sub>3</sub> > toluene) at 298 and 77 K. The results show that the emission peak of compound **1** in solvent exhibits a slight bathochromic shift. However, the emission peaks of compound **1** in CH<sub>3</sub>OH and CHCl<sub>3</sub> are red shift compared with that in CH<sub>3</sub>CN. It is revealed that the luminescence behavior of compound **1** depends on not only the polarity of solvent but also the hydrogen bonding properties between solvent and solute. In addition, the emission peak of compound **1** in solution shows a red shift obviously at 77 K than that at 298 K (*ca.* 144—159 nm), with the fluorescence lifetime increased at 77 K. The lifetime in DMSO at 77 K ( $\tau=12.470$   $\mu\text{s}$ ) was the longest one. The quantum yield of compound **1** increases with increasing the polarity of solvent within a range of 1.8%—8.3 %.

**Keywords** Schiff base; Cd(II)-amine compound; Luminescence; Crystal structure

## 1 Introduction

Coordination polymers have received considerable attention because of their potential application in the fields of gas storage substrate<sup>[1–3]</sup>, molecular absorbent<sup>[4–6]</sup>, ion-exchange material<sup>[7–10]</sup>, heterogeneous catalyst<sup>[11,12]</sup>, and optical material<sup>[13]</sup>. Hitherto, many efforts have been made to carry out the rational design and synthesis of desired and attractive coordination polymers<sup>[14]</sup>. Although significant progress has been achieved in the design and preparation of coordination polymers<sup>[15,16]</sup>, it is still difficult to predict the exact structure of the final product<sup>[17]</sup>. Many factors in the assembly process, such as temperature, reaction duration, counterions, solvents and different conformations of the ligands, finally control the structure of the product<sup>[18–20]</sup>. As is known to all, coordination polymers are usually synthesized by solvothermal reaction at a high temperature and high pressure. The mild reaction conditions have been extensively employed in the construction of discrete complex. In this contribution, we presented the synthesis and detailed structure of one dimension(1D) coordination polymer  $\{[\text{Cd}(\text{mpda})_3] \cdot 2(\text{NO}_3)\}_n$  (**1**) from *m*-phenylenediamine(mpda),

2-acetylpyridine and  $\text{Cd}(\text{NO}_3)_2$  under mild conditions. In addition, in order to study the effects of solvent and temperature on the fluorescence properties of compound **1**, we researched the fluorescence spectra and fluorescence decay curves of it in solid state and solutions, such as dimethyl sulfoxide(DMSO), acetonitrile(CH<sub>3</sub>CN), methyl alcohol(CH<sub>3</sub>OH), trichloromethane(CHCl<sub>3</sub>) and toluene, at 298 and 77 K, and discussed its fluorescent properties in detail.

## 2 Experimental

### 2.1 Materials and General Methods

All the solvents and chemicals used in the synthesis and analysis were commercially obtained and used without further purification. Infrared(IR) spectra were recorded on a Nicolet impact 410 FTIR spectrometer in a range of 4000—400  $\text{cm}^{-1}$  with KBr pellets. Proton nuclear magnetic resonance ( $^1\text{H}$  NMR) spectra were recorded on a Bruker ACF spectrometer at 400 MHz in DMSO-*d*<sub>6</sub> solvent. Chemical shifts( $\delta$ ) were reported with respect to an internal standard of tetramethylsilane(TMS). Elemental analyses for carbon, hydrogen, and nitrogen were

\*Corresponding authors. E-mail: fanruiqing@hit.edu.cn; ylyang@hit.edu.cn

Received January 21, 2014; accepted June 19, 2014.

Supported by the National Natural Science Foundation of China(Nos.21371040, 21171044), the National Key Basic Research Program of China(No.2013CB632900), the Fundamental Research Funds for the Central Universities of China(No.201409) and the Program for Innovation Research of Science in Harbin Institute of Technology, China(Nos.A201416, B201414).

© Jilin University, The Editorial Department of Chemical Research in Chinese Universities and Springer-Verlag GmbH

carried out on a Perkin-Elmer 240C element analyzer. Thermogravimetry(TG) analyses were carried out on a Perkin-Elmer Diamond TG/differential thermal analysis(DTA) instrument thermal analyzer(50—950 °C) in air at a scan rate of 10 °C/min. Ultraviolet-visible(UV-Vis) spectra were obtained on a Perkin-Elmer Lambda 20 spectrometer. Photoluminescence analysis and fluorescence decay curves were recorded on an Edinburgh FLS920 fluorescence spectrometer.

## 2.2 Synthesis of Schiff Base Ligand *N,N'*-Bis(2-pyridinylethylidene)phenylene-1,3-diamine(L)

The acetonitrile solution(10 mL) of mpda(1.0814 g, 10 mmol) was mixed with 2-acetylpyridine(1.4 mL, 20 mmol) for 4 h at 100 °C under stirring. The solution volume was then reduced to 5 mL by evaporation and a brown solution was saved for the further purification. The raw product was purified by column chromatography on a silica-gel column eluted with ethyl acetate/petroleum ether(0/100 to 10/90, volume ratio). The filtrate was evaporated to give a suspension of the product and the pure product L was obtained by filtration, which was washed several times with hexane, and dried in air at ambient temperature.

## 2.3 Synthesis of Compound 1

Ligand L and Cd(NO<sub>3</sub>)<sub>2</sub> in a molar ratio of 1:1 in 30 mL of CH<sub>3</sub>CN were refluxed with stirring for 4 h, then cooled down to room temperature. The bright yellow solution was filtrated and kept for evaporation at room temperature. The needle-like brown crystals were isolated after 7 d. Yield: 20%[based on Cd(NO<sub>3</sub>)<sub>2</sub>]. Elemental anal. calcd. for C<sub>18</sub>H<sub>24</sub>N<sub>8</sub>O<sub>6</sub>Cd(%), found): C 28.55(28.49); H 4.31(4.34); N 19.98(20.02). <sup>1</sup>H NMR(DMSO-d<sub>6</sub>), δ: 6.66(t, 3H, *J*=8.00 Hz), 5.82(s, 3H), 5.80(d, 3H, *J*=4.00 Hz), 5.78(d, 3H, *J*=4.00 Hz), 4.68(s, 12H). IR,  $\tilde{\nu}/\text{cm}^{-1}$ : 3290(s), 3255(s), 3150(m), 3050(m), 2380(w), 1610(s), 1490(s), 1340(vs), 1190(m), 1050(s), 935(s), 866(m), 789(m), 744(w), 698(m), 613(m), 555(m), 459(w), 418(w).

## 2.4 X-Ray Diffraction Analysis

For compound 1 a suitable crystal was coated with hydrocarbon oil and attached to the tip of a glass fiber, which was transferred to a Siemens SMART 1000 CCD diffractometer equipped with graphite-monochromated Mo *K*α radiation ( $\lambda=0.07107$  nm), and operated at (298±2) K. Details of the crystal parameters, data collection and refinement for the structure are collected in Table 1. After data collection, in this case an empirical absorption correction(SADABS) was made<sup>[21]</sup>. And the structure was solved by conventional direct method and refined by full-matrix least squares based on *F*<sup>2</sup> with the help of the SHELXTL 5.1 software package<sup>[22]</sup>. The hydrogen atoms were placed at calculated positions and refined as riding atoms with isotropic displacement parameters. All the non-hydrogen atoms were refined anisotropically. The CCDC 981756 contains the crystallographic data of compound 1. These data can be obtained free of charge at <http://www.ccdc.cam.ac.uk/deposit>. Selected bond lengths and

bond angles of compound 1 are listed in Table S1(see the Electronic Supplementary Material of this paper).

**Table 1 Crystal data and structure parameters for compound 1**

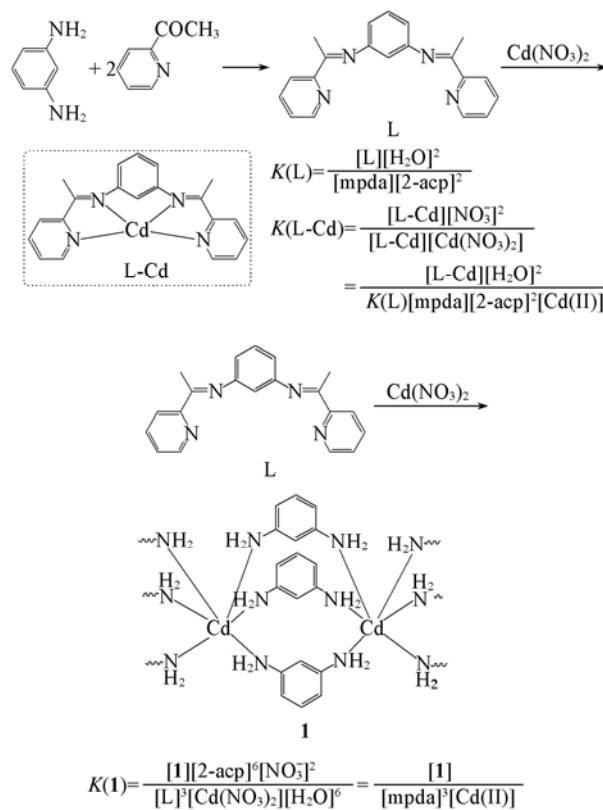
Empirical formula	C <sub>18</sub> H <sub>24</sub> CdN <sub>8</sub> O <sub>6</sub>
Formular weight	560.85
Space group	<i>P6(3)/m</i>
<i>a</i> /nm	0.9126
<i>b</i> /nm	0.9126
<i>c</i> /nm	1.4746
$\alpha$ (°)	90.000
$\beta$ (°)	90.000
$\gamma$ (°)	120.000
<i>V</i> /nm <sup>3</sup>	1.0636(3)
<i>Z</i>	2
<i>T</i> /K	293(2)
$\rho_{\text{calcd.}}$ /(g·cm <sup>-3</sup> )	1.751
$\mu$ /mm <sup>-1</sup>	1.082
$\theta$ range/(°)	3.78—27.48
GOF on <i>F</i> <sup>2</sup>	1.196
Final <i>R</i> index[ <i>I</i> >2σ( <i>I</i> )]	<i>R</i> <sub>1</sub> <sup>a</sup> =0.0239, <i>wR</i> <sub>2</sub> <sup>b</sup> =0.0873
<i>R</i> index(all data) <sup>a</sup>	<i>R</i> <sub>1</sub> =0.0255, <i>wR</i> <sub>2</sub> =0.0891

*a.*  $R_1 = \sum ||F_o| - |F_c|| / \sum |F_o|$ ; *b.*  $wR_2 = \{ \sum [w(F_o^2 - F_c^2)^2] / \sum [w(F_o^2)^2] \}^{1/2}$ .

## 3 Results and Discussion

### 3.1 Synthesis and Characterization

From the Schiff base condensation reaction of mpda with 2-acetylpyridine, we got the Schiff base L which contained a characteristic >C=N— double bond. In the reflux reaction of Schiff base L with Cd(NO<sub>3</sub>)<sub>2</sub>, the Schiff base L decomposed into mpda, forming compound 1. In general, Schiff base



**Scheme 1 Synthetic procedure for compound 1**

would be more stable if one of its substituents is an aromatic group, and it is stable in the solid state or in general organic solvent at room temperature in air. Because of the steric hindrance, methyl group of  $>C=N-$  caused greater torsional tension, which reduced the stability of Schiff base L. Therefore, the more stable structure of compound **1** was formed [Scheme 1,  $K(L)$ ,  $K(L-Cd)$  and  $K(1)$  stand for the reaction equilibrium constants of Schiff base ligand, suspected composition(L-Cd), and compound **1**, respectively]. We failed to use mpda as the only ligand to form compound **1**. This may be due to that mpda appears alkaline in solvent, which makes the metal salt hydrolyzed easily<sup>[23–25]</sup>.

### 3.2 Structure Description

Single crystal X-ray diffraction analysis reveals that compound **1** crystallizes in hexagonal space group  $P6(3)/m$ , as shown in Table 1.

The asymmetric unit contains one sixth Cd(II) ion, half an mpda and one third nitrate anion. The Cd(II) ion lies on the inversion centre, while the six mpdas are separated on two sides of it. As shown in Fig.1, Cd(II) ion is six coordinated by six nitrogen atoms from six independent mpdas. The coordination environment of the Cd(II) center is best described by a slightly distorted octahedron  $[CdN_6]$ . In compound **1**, the six nitrogen atoms are in the same coordination environment, therefore, the Cd—N distances are both 0.2417 nm, which are within the normal distances of those observed in Cd(II)-coordination polymers<sup>[26–30]</sup>. The bond angles around Cd(II) are in a range of  $83.67^\circ$  [ $N1-Cd-N1D(N1F)$ ]— $96.33^\circ$  [ $N1-Cd-N1C(N1E)$ ], and the dihedral angle of the benzene rings is  $60^\circ$ . Because the centre Cd(II) ion is located on the inversion centre, three series of benzene are in the parallel station. The distance between the nearest parallel planes is 0.4080 nm. In compound **1**, adjacent two Cd(II) ions with a Cd···Cd distance of 0.737 nm are bridged with three mpda ligands, generating a 1D chain along  $c$ -axis.

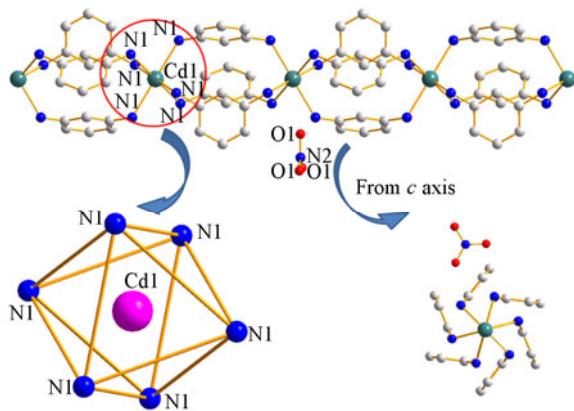


**Fig.1** Ball-and-stick representation of the 1D chain structure of compound **1**, coordination sphere of the  $Cd^{2+}$  centre with a distorted octahedral geometry and triple axis of rotation along the  $c$  axis in compound **1**

The intermolecular interactions play a significant role in

the packing of the crystals. As shown in Fig.2, there are  $N1-H1B\cdots O(146.79^\circ)$  and  $N1-H1C\cdots O(169.33^\circ)$  hydrogen bonding interactions, with the distances of 0.3151 and 0.3166 nm. Each oxygen atom of every nitro is in the formation of hydrogen bonds with the different hydrogen atoms of two amino groups. The angle of nitro group deviated from benzene ring of mpda is  $90^\circ$ , which makes the molecule have a vertical and horizontal interlaced structure. The 1D chains are further assembled into a 3D supramolecular network *via* hydrogen bonding interactions (Table S2, see the Electronic Supplementary Material of this paper), contributing to the additional stability of the structure.

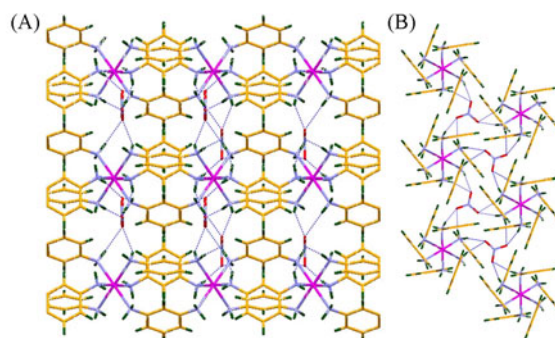


**Fig.2** Packing diagram of compound **1** along  $b$  axis(A) and  $c$  axis(B)

Hydrogen bonds are indicated by dashed line.

### 3.3 IR Spectra of Compound 1

The IR spectra of mpda and compound **1** are shown in Fig.S1 (see the Electronic Supplementary Material of this paper). The absorption bands of mpda in the compound are shifted to lower wavenumbers by  $25\text{ cm}^{-1}$  compared with those of the free mpda ligand, which is consistent with the coordination of mpda to the metal ion center *via* the amino nitrogen atoms<sup>[31]</sup>. In the IR spectrum of compound **1**, the absorption bands centered at  $3290$  and  $3255\text{ cm}^{-1}$  are attributed to N—H bonds asymmetric and symmetric stretching vibrations, respectively. The band at  $3150\text{ cm}^{-1}$  is associated with the stretching vibrations of C—H bonds of benzene ring, which appears at  $3210\text{ cm}^{-1}$  in free mpda. Characteristic bands of benzene ring appear at  $1900$ — $1700$  and  $900$ — $700\text{ cm}^{-1}$  in the spectrum of compound **1**. The bending vibration bands of the benzene ring in compound **1** have shifted towards lower frequencies compared to those in mpda, which indicates that there exist intermolecular or intramolecular hydrogen bond interactions in the solid state of compound **1**. This kind of non-covalent bond could inhibit the molecular vibration<sup>[32]</sup>, which was further confirmed by single-crystal X-ray diffraction analysis.

### 3.4 $^1H$ NMR Spectra of Compound 1

The  $^1H$  NMR spectroscopy was used for the confirmation of mpda bound to the metal ion for compound **1**, which is illustrated in Fig.S2 (see the Electronic Supplementary Material of this paper). The  $^1H$  NMR spectrum of compound **1** in DMSO- $d_6$  exhibits a singlet peak at  $\delta$  4.68 assigned to amino protons ( $-NH_2$ ). It is shifted to the downfield region compared

with that of free mpda, indicating the coordination between the metal ion and ligand. For compound **1**, the signal of the aromatic hydrogen H1A split by H2A atoms is considered as a triplet at  $\delta$  6.66. This signal of free mpda shifts to  $\delta$  6.91. The signal of H2A atoms was observed as a doublet at  $\delta$  5.80 and 5.78 with a coupling constant of 4.00 Hz due to the coupling with H1A. In free mpda, this doublet appeared at  $\delta$  6.076. H3A exhibited a triplet at  $\delta$  5.82, while that of mpda exhibited a triplet at  $\delta$  5.944.

### 3.5 Spectral Behavior of Compound **1** in Different Solvents

The absorption spectra of compound **1** and mpda were investigated in different solvents (polarity: DMSO > CH<sub>3</sub>CN > CH<sub>3</sub>OH > CHCl<sub>3</sub> > toluene). The emission spectra of compound **1** and mpda in solid state are shown in Table S3 and Fig.S3 (see the Electronic Supplementary Material of this paper). And mpda shows similar spectral properties as compound **1**. Typical absorption spectra of compound **1** in different solvents are shown in Fig.3. The corresponding maximum absorption wavelength and molar extinction coefficients ( $\epsilon$ ) values are given in Table S4 (see the Electronic Supplementary Material of this paper). The absorption maximum of compound **1** was observed to shift from 292 nm to 303 nm obviously with the increased solvent polarity from CH<sub>3</sub>OH to DMSO, corresponding to  $\pi \rightarrow \pi^*$  electronic transition of the aromatic rings. And the maximum molar extinction coefficient ( $\epsilon$ ) value is  $0.74 \times 10^5$  L/(mol·cm) in DMSO. According to modern molecular orbital theory,<sup>[33]</sup> any factors that can influence the electronic density of a conjugated system must result in the bathochromic or hypsochromic shift of the absorption band<sup>[34]</sup>. The bathochromic shift of compound **1** in polar solutions implies that the value of dipole moment is higher in the excited state structure than in ground state, so the excited state is more sensitive than ground state. With the increasing of solvent polarity, excited state  $\pi^*$  is to be more stable than ground state  $\pi$ . Thus in more polar solvents, the excited state is at lower energy level, which reduces the energy difference between ground state and excited state. Therefore, the absorption peak is red shifted with the increase of solvent polarity. However, the absorption spectrum of compound **1** in CHCl<sub>3</sub> and toluene does not follow this rule. It may be due to that the weak or non-polar solvent could not influence the electronic density of a conjugated system and is

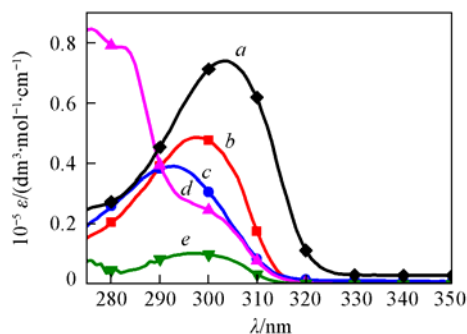


**Fig.3** UV-Vis spectra of compound **1** in different solvents ( $c=10^{-5}$  mol/L) at 298 K  
a. DMSO; b. CH<sub>3</sub>CN; c. CH<sub>3</sub>OH; d. CHCl<sub>3</sub>; e. toluene.

unable to result in the bathochromic or hypsochromic shift of the absorption band.

The coordination polymers of  $d^{10}$  metal centre have been investigated for fluorescence properties owing to their potential application in photoactive materials<sup>[35–41]</sup>. The photoluminescence properties of compound **1** were studied in DMSO, CH<sub>3</sub>CN, CH<sub>3</sub>OH, CHCl<sub>3</sub>, toluene solvents at the same concentration ( $1.0 \times 10^{-5}$  mol/L) (Fig.4). The mpda ligand has a similar photoluminescence properties to compound **1** (Fig.S4, see the Electronic Supplementary Material of this paper). It is shown that compound **1** displays bluish violet fluorescence emission in these aprotic or protic solvents in a region of 325–337 nm. Since it is difficult to oxidize or reduce the Cd(II) cations due to their  $d^{10}$  configuration<sup>[42–44]</sup>, the origin of the emission for compound **1** is neither metal-to-ligand charge transfer (MLCT) nor ligand-to-metal charge transfer (LMCT). The intense fluorescent emission of compound **1** is attributed to the intraligand  $\pi^* \rightarrow \pi$  transition of mpda ligand. Effect of solvent polarity on the emission spectrum of compound **1** is obvious in the aprotic or protic solvents at 298 K. On going from toluene to DMSO, the emission band of compound **1** displays a red shift from 325 nm to 337 nm. The photoluminescence emission peak of compound **1** apparently displays a red shift with the increased solvent polarity. It is attributed to the fact that the ground-state energy distribution is not affected to a greater extent possibly due to the less polar nature than that in excited state<sup>[45]</sup>. Therefore, the emission peak is sensitive to the polarity of medium. Although CH<sub>3</sub>CN possesses a more strong polarity than CH<sub>3</sub>OH and CHCl<sub>3</sub>, the fluorescence emission peak in the latter solvents performs red shift with respect to it in CH<sub>3</sub>CN solvent, which is from 329 nm in CH<sub>3</sub>CN to 332 nm in CH<sub>3</sub>OH and 331 nm in CHCl<sub>3</sub> upon excitation at 300 nm. Meanwhile, the emission band of compound **1** in CHCl<sub>3</sub> is broader. It may be due to the active hydrogen of amino in compound **1**, which could form hydrogen bond with chlorine atoms of CHCl<sub>3</sub> and oxygen atom in CH<sub>3</sub>OH. The hydrogen bond seems to stabilize the excited state by solute-solvent interactions.

The change of temperature from 298 K to 77 K<sup>[46–49]</sup> caused the red shift of the emission peak (*ca.* 144–159 nm) substantially in all the solutions of compound **1**, and the emission peak show rich structural features at 77 K. In the CH<sub>3</sub>CN solution, the emission band of compound **1** is red shift from 329 nm to 488 nm (*ca.* 159 nm) from 298 K to 77 K. Such fascinating phenomenon may be attributed to the different state of solution at the low temperature. At 77 K, the viscosity of the solvent increases, and the interaction between fluorescent substance and solvent, the forces of attraction and hydrogen bonds may be stronger in contrast with those at 298 K. In this case, excited state is more stable, and the energy level difference between ground state and excited state decreases. Accordingly, the fluorescence emission peak of compound **1** in solution displays a red shift significantly from 298 K to 77 K.

The fluorescence quantum yields ( $\Phi_f$ ) of compound **1** were determined in diluted DMSO, CH<sub>3</sub>CN and CH<sub>3</sub>OH solutions ( $1.0 \times 10^{-5}$  mol/L). Quinine sulphate with known quantum yield acts as reference fluorophore. Equation(1) was used for calculating the quantum yield:

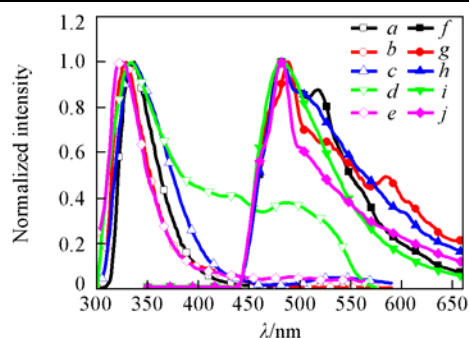


**Fig.4** Normalized emission spectra of compound **1** in different solvent( $c=10^{-5}$  mol/L) at 298 and 77 K

*a.* DMSO, 298 K; *b.* CH<sub>3</sub>CN 298 K; *c.* CH<sub>3</sub>OH, 298 K; *d.* CHCl<sub>3</sub>, 298 K; *e.* toluene, 298 K; *f.* DMSO, 77 K; *g.* CH<sub>3</sub>CN, 77 K; *h.* CH<sub>3</sub>OH, 77 K; *i.* CHCl<sub>3</sub>, 77 K; *j.* toluene, 77 K.

$$\frac{\Phi_{\mu}}{\Phi_s} = \frac{F_{\mu} A_s n_{\mu}^2}{F_s A_{\mu} n_s^2} \quad (1)$$

in which subscripts  $\mu$  and  $s$  refer to the sample of the tested compound (with unknown quantum yield) and the reference fluorophore,  $F$  is the area under the fluorescent emission curve,  $A$  denotes the absorbance at the wavelength of excitation and  $n$  is the refractive index of the solvent<sup>[50]</sup>. The values of the quantum yields for compound **1** in DMSO, CH<sub>3</sub>CN and CH<sub>3</sub>OH are 0.083, 0.029 and 0.18, respectively, which is increased with the increased polarity of the solvents (polarity: DMSO > CH<sub>3</sub>CN > CH<sub>3</sub>OH).

The fluorescence lifetimes of compound **1** and mpda in solution were measured at 298 and 77 K, respectively, which are shown in Fig.5. The decay curve is well fitted into a double exponential function<sup>[51–53]</sup>:

$$I = I_0 + A_1 \exp(-t/\tau_1) + A_2 \exp(-t/\tau_2) \quad (2)$$

where  $I$  and  $I_0$  are the luminescent intensities at time  $t=t$  and  $t=0$ , respectively, whereas  $\tau_1$  and  $\tau_2$  are defined as the luminescent lifetime. The average lifetimes were calculated according to the following Eq.(3) with the results listed in Table S4 (see the Electronic Supplementary Material of this paper):

$$\tau = \frac{\tau_1^2 A_1 + \tau_2^2 A_2}{\tau_1 A_1 + \tau_2 A_2} \quad (3)$$

The double exponential fluorescence decay indicates that mpda ligand and compound **1** have two independent excited states each. Each state possesses the characteristic lifetime, which could contribute the process of fluorescence decay. It is shown that the lifetimes of compound **1** and mpda ligand in solution do not strongly depend on the property of solvent but on the temperature. The luminescent lifetimes for compound **1** and mpda in solutions at 77 K are mostly longer than those at 298 K. Particularly, the lifetime of compound **1** in CHCl<sub>3</sub> at 77 K ( $\tau=12.293 \mu\text{s}$ ) is 1.94 folds that at 298 K ( $\tau=6.323 \mu\text{s}$ ), and the lifetime of mpda in DMSO at 77 K ( $\tau=10.528 \mu\text{s}$ ) is 1.76 folds to that at 298 K ( $\tau=5.968 \mu\text{s}$ ). These features might be ascribed to an increased contribution from delayed fluorescence which was caused by excimer formation at liquid nitrogen temperature<sup>[46–49]</sup>. Moreover, the lower temperature limited the lost of non-radiative transitions of molecules. The thermogravimetric curves showed that compound **1** start to undergo phase

transition until *ca.* 230 °C, which induces the structure collapse (Fig.S5, see the Electronic Supplementary Material of this paper).

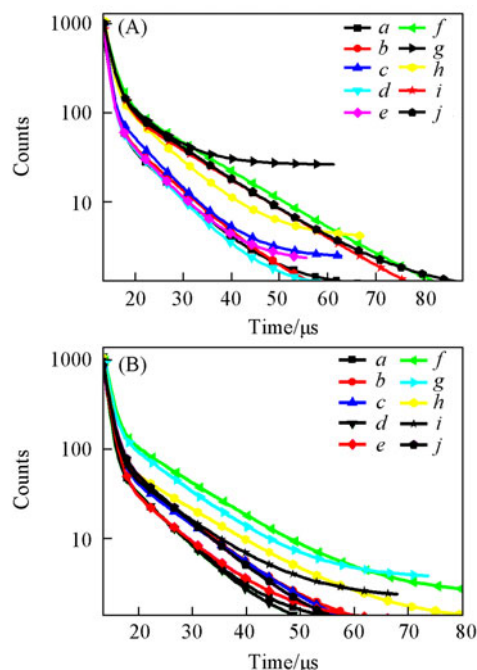


**Fig.5** Luminescence decay profiles of compound **1**(A) and mpda ligand(B) at 298 and 77 K

*a.* DMSO, 298 K; *b.* CH<sub>3</sub>CN 298 K; *c.* CH<sub>3</sub>OH, 298 K; *d.* CHCl<sub>3</sub>, 298 K; *e.* toluene, 298 K; *f.* DMSO, 77 K; *g.* CH<sub>3</sub>CN, 77 K; *h.* CH<sub>3</sub>OH, 77 K; *i.* CHCl<sub>3</sub>, 77 K; *j.* toluene, 77 K.

## 4 Conclusions

Compound **1** was successfully synthesized from ligand L and Cd(NO<sub>3</sub>)<sub>2</sub> under refluxing in acetonitrile and its single crystal structure was confirmed by X-ray diffraction analysis. In the crystal structure of compound **1**, two adjacent Cd(II) ions were linked by three mpda to form a 1D chain, constituting a triple rotation axis. Furthermore, there are significant non-covalent interactions of N—H···O, on account of which a 3D feature structure of compound **1** was formed. At 298 K, compound **1** exhibits the intense blue-violet fluorescent emission in the aprotic or protic solutions ( $\lambda_{em}=325\text{—}337 \text{ nm}$ ), which is sensitive to the polarity of the medium. The change of temperature from 298 K to 77 K led to the red shift of the emission peak (*ca.* 144—159 nm) in all the solutions of compound **1**. Interestingly, the fluorescence lifetime of compound **1** in different solutions is not strongly dependent on solvent but on temperature. The longest fluorescence lifetime of compound **1** in solution is 12.293  $\mu\text{s}$  measured in CHCl<sub>3</sub> at 77 K. The superior luminescence properties make compound **1** a promising material for the development of optical devices.

## Electronic Supplementary Material

Supplementary material is available in the online version of this article at <http://dx.doi.org/10.1007/s40242-014-4032-z>.

## References

- [1] Murray L. J., Dinca M., Long J. R., *Chem. Soc. Rev.*, **2009**, *38*, 1294
- [2] Wang Y. Y., Zhang Z., Sun Y. J., *Chem. J. Chinese Universities*, **2014**, *35*(3), 449
- [3] Huang Q. D., Li C. L., Zhang Y., *Chem. J. Chinese Universities*, **2014**, *35*(3), 524
- [4] Li J. R., Kuppler R. J., Zhou H. C., *Chem. Soc. Rev.*, **2009**, *38*, 1477
- [5] Shi W. B., Kou H. Z., *Chem. J. Chinese Universities*, **2014**, *35*(1), 12
- [6] Lu W. G., Liu H. W., Yin X. G., *Chem. J. Chinese Universities*, **2013**, *34*(12), 2691
- [7] Plabst M., McCusker L. B., Bein T., *J. Am. Chem. Soc.*, **2009**, *131*, 18112
- [8] Liu Y., Kravtsov V. C., Eddaoudi M., *Angew. Chem., Int. Ed.*, **2008**, *47*, 8446
- [9] Monika P., McCusker L. B., Bein T., *J. Am. Chem. Soc.*, **2009**, *131*, 18112
- [10] Liu H. W., Chen X. F., Zhang J., *Acta Polymeric Sinica*, **2014**, *1*, 115
- [11] Lee J. Y., Farha O. K., Roberts J., Scheidt K. A., Nguyen S. T., Hupp J. T., *Chem. Soc. Rev.*, **2009**, *38*, 1450
- [12] Ma L., Abney C., Lin W., *Chem. Soc. Rev.*, **2009**, *38*, 1248
- [13] Allendorf M. D., Bauer C. A., Bhakta R. K., Houk R. J. T., *Chem. Soc. Rev.*, **2009**, *38*, 1330
- [14] Wu D. Q., Meng W., Zhang L., Liu L., Hou H. W., Fan Y. T., *Inorg. Chim. Acta*, **2013**, *405*, 318
- [15] Friedrichs O. D., O'Keefe M., Yaghi O. M., *Acta Crystallogr.*, **2003**, *A59*, 22
- [16] Friedrichs O. D., O'Keefe M., Yaghi O. M., *Acta Crystallogr.*, **2003**, *A59*, 515
- [17] Qi Y., Luo F., Che Y. X., Zheng J. M., *Cryst. Growth Des.*, **2008**, *8*, 606
- [18] Tong M. L., Ye B. H., Cai J. W., Chen X. M., Ng S. W., *Inorg. Chem.*, **1998**, *37*, 2645
- [19] Hennigar T. L., MacQuarrie D. C., Losier P., Rogers R. D., Zawrotko M. J., *Angew. Chem., Int. Ed. Engl.*, **1997**, *36*, 972
- [20] Zhang W. L., Liu Y. Y., Ma J. F., Jiang H., Yang J., Ping G. J., *Cryst. Growth Des.*, **2008**, *8*, 1250
- [21] Sheldrick G. M., *Software for Data Extraction and Reduction, Version 6.02*, Bruker Axs Inc., Madison, WI, **2002**
- [22] Sheldrick G. M., *SHELXTL NT Crystal Structure Analysis Package, Version 5.10*, Bruker Axs Inc., Madison, WI, **1999**
- [23] Duliban J., *J. Appl. Polym. Sci.*, **2012**, *125*, 3708
- [24] Mbuli B. S., Dlamini D. S., Nxumalo E. N., Krause R. W., Pillay V. L., Oren Y., Linder C., Mamba B. B., *J. Appl. Polym. Sci.*, **2013**, *129*, 549
- [25] Idris A., Kormin F., Noordim M. Y., *Separation and Purification Technology*, **2006**, *49*, 271
- [26] Lin J. D., Cheng J. W., Du S. W., *Cryst. Growth Des.*, **2008**, *8*, 3345
- [27] Zhang L. P., Yang J., Ma J. F., Jia Z. F., Xie Y. P., Wei G. H., *Cryst. Eng. Comm.*, **2008**, *10*, 1395
- [28] Habib H. A., Sanchiz J., Janiak C., *Dalton Trans.*, **2008**, 1734
- [29] Ren P., Liu M. L., Zhang J., Shi W., Cheng P., Liao D. Z., Yan S. P., *Dalton Trans.*, **2008**, 4711
- [30] Hsu Y. F., Hu H. L., Wu C. J., Yeh C. W., Proserpioc D. M., Chen J. D., *Cryst. Eng. Comm.*, **2009**, *11*, 122
- [31] Shi X. J., Wang X., Li L., Hou H. W., Fan Y. T., *Cryst. Growth Des.*, **2010**, *10*, 2490
- [32] Kosar B., Albayrak C., Ersanli C. C., Odabasoglu M., Buyukgungor O., *Spectrochim. Acta A*, **2012**, *93*, 1
- [33] Kasumov V. T., *Spectrochim. Acta A*, **2003**, *57*, 1649
- [34] Ceyhan G., Köse M., Tümer M., Demirtaş İ., Yağlıoğlu A. Ş., McKee V., *J. Luminescence*, **2013**, *143*, 623
- [35] Lu J., Li Y., Zhao K., Xu J. Q., Yu J. H., Li G. H., Zhang X., Bie H. Y., Wang T. G., *Inorg. Chem. Commun.*, **2004**, *7*, 1154
- [36] Zhang C. M., Lin J., *Chem. Soc. Rev.*, **2009**, *8*, 1330
- [37] Yao X. Q., Zhang M. D., Hu J. S., Li Y. Z., Guo Z. J., Zheng H. G., *Cryst. Growth Des.*, **2011**, *11*, 3039
- [38] Lan A. J., Li K. H., Wu H. H., Olson D. H., Emge T. J., Ki W., Hong M. C., Li J., *Angew. Chem., Int. Ed.*, **2009**, *48*, 2334
- [39] Zang S. Q., Su Y., Li Y. Z., Lin J. G., Duan X. Y., Meng Q. J., Gao S., *Cryst. Eng. Comm.*, **2009**, *11*, 122
- [40] Habib H. A., Hoffmann A., Höpfe H. A., Steinfeld G., Janiak C., *Inorg. Chem.*, **2009**, *48*, 2166
- [41] Liu W. L., Ye L. H., Liu X. F., Yuan L. M., Jiang J. X., Yan C. G., *Cryst. Eng. Comm.*, **2008**, *10*, 1395
- [42] Wen L. L., Dang D. B., Duan C. Y., Li Y. Z., Tian Z. F., Meng Q. J., *Inorg. Chem.*, **2005**, *44*, 7161
- [43] Hu T. L., Zou R. Q., Li J. R., Bu X. H., *Dalton Trans.*, **2008**, 1302
- [44] Zencirci N., Gelbrich T., Apperley D. C., Harris R. K., Kahlenberg V., Griesser U. J., *Cryst. Growth Des.*, **2010**, *10*, 303
- [45] Wang X. M., Qiang L. S., Fan R. Q., Wang P., Yang Y. L., *Supramolecular Chem.*, **2013**, *25*, 416
- [46] Dijken A. V., Meulenkaamp E. A., Vanmaekelbergh D., Meijerink A., *J. Phys. Chem. B*, **2000**, *104*, 1715
- [47] Constable E. C., Neuburger M., Rösel P., Schneider G. E., Zampese J. A., Housecroft C. E., Monti F., Armaroli N., Costa R. D., Orti E., *Inorg. Chem.*, **2013**, *52*, 885
- [48] Ivanov P., Stanimirov S., Kaloyanova S., Petkov I., *J. Fluoresc.*, **2012**, *22*, 1501
- [49] Dobek K., Karoleczak J., *J. Fluoresc.*, **2012**, *22*, 1647
- [50] Kubinyi M., Varga O., Baranyai P., Kállay M., Mizsei R., Tárkányi G., Vidóczy T., *J. Mol. Struct.*, **2011**, *1000*, 77
- [51] Rodríguez-Diéguez A., Salinas-Castillo A., Sironi A., *Cryst. Eng. Comm.*, **2010**, *12*, 1876
- [52] Fan R. Q., Zhang Y. J., Yin Y. B., Su Q., Yang Y. L., Hasi W., *Syn. Met.*, **2009**, *159*, 1106
- [53] Murugan K. D., Natarajan P., *Eur. Polym. J.*, **2011**, *47*, 16